A Novel Parallel Concatenated Convolutional Code Structure Based on Frame Decomposition

Mohammad Bazzal, Jérémy Nadal, Stefan Weithoffer, Charbel Abdel Nour, Catherine Douillard

▶ **To cite this version:**

Mohammad Bazzal, Jérémy Nadal, Stefan Weithoffer, Charbel Abdel Nour, Catherine Douillard. A Novel Parallel Concatenated Convolutional Code Structure Based on Frame Decomposition. ISTC 2025: International Symposium on Topics in Coding, Aug 2025, Los angeles, CA, United States. ⟨hal-05168399⟩

HAL Id: hal-05168399

https://imt-atlantique.hal.science/hal-05168399v1

Submitted on 17 Jul 2025

HAL is a multi-disciplinary open access archive for the deposit and dissemination of scientific research documents, whether they are published or not. The documents may come from teaching and research institutions in France or abroad, or from public or private research centers.

L'archive ouverte pluridisciplinaire **HAL**, est destinée au dépôt et à la diffusion de documents scientifiques de niveau recherche, publiés ou non, émanant des établissements d'enseignement et de recherche français ou étrangers, des laboratoires publics ou privés.

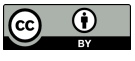

Distributed under a Creative Commons CC BY 4.0 - Attribution - International License

A Novel Parallel Concatenated Convolutional Code Structure Based on Frame Decomposition

Mohammad Bazzal, Jeremy Nadal, Stefan Weithoffer, Charbel Abdel Nour, Catherine Douillard
IMT Atlantique, Lab-STICC, UMR CNRS 6285, F-29238 Brest, France

***Abstract*—This paper introduces a novel decomposed parallel concatenated convolutional code (DPCCC) structure designed to increase the minimum Hamming distance (mHD) and reduce the error floor compared to conventional PCCC structures, such as turbo codes (TCs). In DPCCC, the input frame is partitioned into subframes, each independently interleaved and encoded. This decomposition targets mHD codewords, partly through mitigating the quadratic increase in the multiplicity of periodic input weight-2 sequences, thus lowering their probability of co-occurrence in the component codes. We also propose a design algorithm that optimizes each subframe interleaver while accounting for inter-frame dependencies. Simulation results demonstrate that the proposed DPCCC structure, combined with the tailored interleaver design, achieves competitive performance compared to other code classes, with notable improvements in mHD and error floor performance over TCs, while maintaining rate compatibility and supporting low-latency decoder architectures.**

***Index Terms*—Turbo codes, interleaver, return-to-zero sequence, minimum Hamming distance, error floor.**

I. Introduction

Turbo codes (TCs) have played a crucial role in the evolution of modern communication systems, offering near-capacity error correction performance [1]. They are based on the parallel concatenation of convolutional codes (CCs), where recursive systematic convolutional (RSC) encoders are interconnected via interleavers to mitigate correlated errors [2]. In contrast to parallel concatenated CCs (PCCCs), serial concatenated CCs (SCCCs) typically provide larger minimum Hamming distances (mHD) but underperform at low signal-to-noise ratios (SNRs) [3]. TCs remain widely adopted, including in standards such as LTE Advanced Pro [4].

At high SNRs, the error correction performance of conventional TCs is constrained by their mHD, with low distances leading to high error floors [5]. Accurate mHD estimation is therefore essential but remains a significant challenge in TC design. Traditional techniques—such as the simple impulse method (SIM), double impulse method (DIM), and event impulse method (EVIM) [6]—approximate the mHD by analyzing decoder responses to injected impulsive errors. However, these approaches are computationally intensive and inherently decoder-dependent, hindering their accuracy. To address this limitation, we recently introduced a decoder-independent, computationally efficient approach based on the identification of return-to-zero (RTZ) sequences [7]. This method exploits the properties of turbo RTZ (TRTZ) sequences—RTZ sequences for both component codes with the same input weight (IW)—to build a graph-based framework for mHD evaluation. Furthermore, it supports on-the-fly estimation during interleaver design by utilizing partial interleaver connections, thereby enabling more effective code constructions.

This work was supported by the Agence Nationale de la Recherche (ANR) under the France 2030 program, grant "NF-PERSEUS : ANR-22-PEFT-0004".

Building on these recent insights into TRTZ sequences, this work introduces a novel decomposed PCCC (DPCCC) structure, detailed in Section III. By dividing the input frame into smaller subframes that are independently interleaved and encoded, the DPCCC scheme effectively suppresses the emergence of low-weight TRTZ sequences, as shown in Section IV. An iterative interleaver design strategy is also proposed to account for subframe interactions and their influence on the occurrence of TRTZ sequences. This combined approach enhances the mHD and lowers the error floor, leading to notable performance gains at high SNRs, as demonstrated in Section V.

II. Background on PCCCs and TRTZ sequences

In PCCC schemes, as illustrated in Fig. 1, each RSC component encoder C_q ($q \in [1, n_{cc}]$) processes a permuted version of the input sequence $\mathbf{d}_q$ of length K, as defined by interleaver Π_q. This permutation ensures that each encoder receives a distinct rearrangement of the input, thereby reducing error correlation. Following encoding, the overall code rate is adjusted by applying a puncturing mask $\mathcal{P}_q$ to selectively omit parity bits from transmission.

Due to the linearity of CCs, their distance spectrum can be evaluated by analyzing the Hamming weights of non-zero codewords. In practice, this involves traversing the code trellis to enumerate sequences that diverge from and return to the zero state—referred to as RTZ sequences. For recursive CCs, the Hamming weight of an RTZ sequence is constrained by its length, motivating a focus on short RTZ sequences. The mHD, also known as the free distance of the code [8], corresponds to the RTZ sequence with the lowest Hamming weight [8]. Let R denote an RTZ sequence with IW w, defined as:

$$R = \{x_0, x_1, \ldots, x_{w-1}\}, \tag{1}$$

where $x_0, x_1, \ldots, x_{w-1}$ indicate the bit indices of the '1's relative to the start of the RTZ sequence. For an RSC code, any RTZ sequence of IW $w = 2$ can be described as:

$$\{x_0, x_1\} \quad \text{with} \quad |x_0 - x_1| \bmod p = 0, \tag{2}$$

where p is the length of the shortest RTZ sequence of the code with $w = 2$, also known as the period of the RSC code.

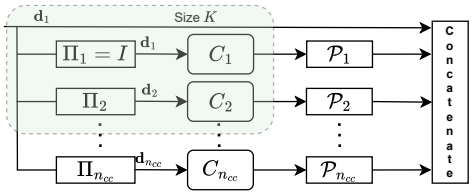

Fig. 1: General structure of a parallel concatenated convolutional code. Shaded area: special case of a TC.

The *Reduction* operation F_R that yields a reduced sequence of at most length p, takes the modulo p of each element in the original sequence $S = \{s_i\}_{i \in [\![0, w-1]\!]}$ and removes all pairwise repetitions. For two sequences (S_1, S_2), let $S_1 \uplus S_2$ denote the symmetric difference of their union, expressed as:

$$S_1 \uplus S_2 = (S_1 \cup S_2) \setminus (S_1 \cap S_2). \tag{3}$$

Using this, the reduction operation F_R can be written as:

$$F_R(S) = \biguplus_{i=1}^{|S|} \{s_i \bmod p\}, \tag{4}$$

where $|.|$ denotes the cardinality of a set, and $|S|$ represents the number of bits equal to '1' in the sequence.

Theorem 1 from [7] provides the following criterion for determining whether a given sequence qualifies as an RTZ sequence:

Theorem 1: A sequence S is an RTZ sequence if, and only if, its reduction under the operation F_R results in a sequence that belongs to the atomic set RTZ_a or the empty set $\emptyset$:

$$F_R(S) \in (RTZ_a \cup \{\emptyset\}) \Leftrightarrow S \text{ is an RTZ sequence.} \tag{5}$$

Here, the atomic set RTZ_a is defined as the set of all possible RTZ sequences within a single period p, i.e all RTZ sequences with length $\leq p$:

$$RTZ_a = \{R : 0 \leq w < p,\ 0 \leq x_i < p\}. \tag{6}$$

RTZ_a can be easily enumerated by encoding the non-zero $2^p - 1$ input sequences R and collecting the ones that classify as an RTZ. Inversely, any RTZ sequence $R_i \notin RTZ_a$ can be expressed as the symmetric difference of a base atomic RTZ $R_j \in RTZ_a$ and a set of IW-2 RTZ sequences:

$$R_i = R_j \uplus \biguplus_k R_k^{(2)}, \tag{7}$$

where each $R_k^{(2)}$ is an IW-2 RTZ sequence. Hence, the cardinality of the full RTZ set is largely impacted by the cardinality of the IW-2 subset.

We extend the concept of RTZ sequences to the parallel concatenation of multiple RSC encoders. A TRTZ sequence is defined as a sequence that satisfies the RTZ condition simultaneously across all component encoders. Accordingly, the IW w of a TRTZ sequence matches the IW of each individual component RTZ sequence. At high SNRs, the performance of PCCCs is primarily limited by low-IW TRTZ sequences, which produce low total Hamming weights—also referred to as output weights (OWs) [7]. In particular, due to the periodicity of the recursive polynomial, the number of IW $w = 2$ sequences grows exponentially with frame size, causing increasing difficulty for the interleaver to suppress them effectively.

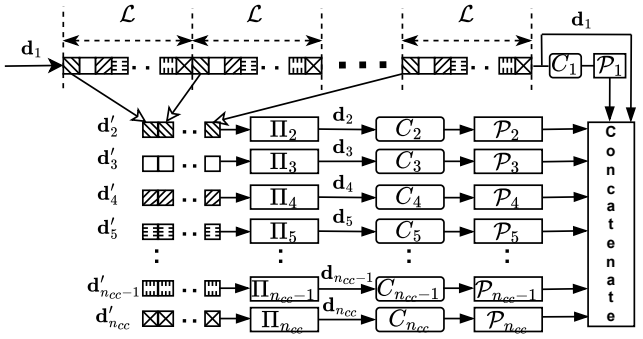

Fig. 2: Overview of the proposed DPCCC structure.

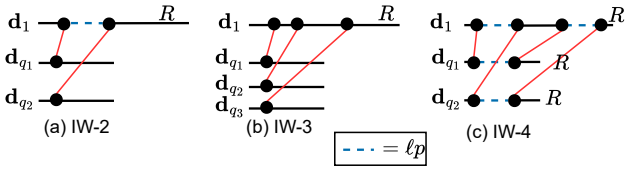

Fig. 3: Decomposition of different sequences with varying IWs. Dashed line: spatial distance between two bits is a multiple of p.

III. Proposed New DPCCC Structure

To mitigate the occurrence of low-IW TRTZ sequences thereby improving the mHD of the code, we propose a structural modification illustrated in Figure 2, referred to as DPCCC. In this structure, the first parity output of length K is generated by encoding the original information frame $\mathbf{d}_1$ using encoder C_1. The frame $\mathbf{d}_1$ is then uniformly partitioned into $\mathcal{L} = n_{cc} - 1$ subframes, denoted by $(\mathbf{d}'_2, \ldots, \mathbf{d}'_{n_{cc}})$, as shown in Figure 2.

Each subframe $\mathbf{d}'_q$ ($q \in [2, n_{cc}]$) is formed by selecting bits from $\mathbf{d}_1$ according to the following indexing rule:

$$\mathbf{d}'_q[\ell] = \mathbf{d}_1[\ell\mathcal{L} + q - 2],\ \forall \ell < K/\mathcal{L} - 1 \tag{8}$$

Each subframe $\mathbf{d}'_q$ is interleaved using Π_q to produce $\mathbf{d}_q$, which is subsequently encoded by constituent encoder C_q using tailbiting termination. The size of each decomposed subframe $\mathbf{d}'_q$ is given by $\lfloor K/\mathcal{L} \rfloor$. The overall code rate, without puncturing, is $1/3$, comprising K bits from the systematic stream, K from the first parity, and K from all subframe parities—matching the rate of conventional TCs.

To support higher code rates, appropriate puncturing masks can be applied. For lower code rates ($\mathcal{R} \leq 1/3$), the subframe size can be increased to $\alpha K/\mathcal{L}$, where $\alpha = 1/\mathcal{R} - 2$, by extracting additional bits from $\mathbf{d}_1$. This approach ensures rate flexibility while preserving the structural advantages of the decomposition. Therefore, the DPCCC scheme is fully defined by the number of decompositions $\mathcal{L}$ and tuple $\delta = (\Pi_q, C_q, \mathcal{P}_q)_{q \in [1, n_{cc}]}$, where Π_1 is the identity interleaver I.

We define the decomposition operation F_D as a mapping that takes a sequence S from the main frame $\mathbf{d}_1$ and returns a tuple of decomposed sets $S_D = (S_2, \ldots, S_{n_{cc}})$. Each S_j represents the set of indices projected into subframe $\mathbf{d}_j$ according to the decomposition rule in (8), Formally:

$$S_j = \bigcup \left\{ \left\lfloor \frac{s_i}{\mathcal{L}} \right\rfloor \,\middle|\, s_i \in S,\, j = (s_i \bmod \mathcal{L}) + 2 \right\} \tag{9}$$

For indices S $\in S_D$ that do not map to a given subframe, the corresponding set S_j is empty.

Consequently, a TRTZ sequence T in the DPCCC scheme can be described as an RTZ sequence in $\mathbf{d}_1$ such that $S_D = F_D(T)$ satisfies the RTZ condition in every subframe, as follows:

$$\forall S_j \in S_D, \quad F_R(S_j) \in (\textit{RTZ}_a \cup \{\emptyset\}), \tag{10}$$

where F_R is the reduction operation defined in (4).

The objective is then to find $\delta^\star$ such that

$$\delta^\star = \underset{\mathcal{L},\delta}{\operatorname{argmax}} \left(\min_{T \in \mathcal{T}} W(T) \right), \tag{11}$$

where $\mathcal{T}$ represents the set of all TRTZ sequences for a given DPCCC configuration, and $W(\cdot)$ computes their OW after encoding with the DPCCC.

This optimization problem is inherently complex due to its multidimensional nature, involving choices of encoder polynomials, puncturing masks, and decomposition size $\mathcal{L}$. As a initial approach, we adopt CC parameters and puncturing masks from prior art, focusing the search on the optimal decomposition $\mathcal{L}$. Subsequently, we employ an iterative interleaver design strategy to further enhance performance.

IV. Proposed Design Methodology

This section presents a methodology for determining a suitable value for $\mathcal{L}$ based on its impact on performance through the TRTZ sequences. We also propose an interleaver design strategy for DPCCC aimed at maximizing the mHD.

A. Analysis of TRTZ sequences

We categorize TRTZ sequences into two distinct types:

1) Single-layer TRTZ sequences (TRTZ$_{sl}$): defined as TRTZ sequences T where the RTZ sequence in $\mathbf{d}_1$ decomposes into an RTZ sequence in exactly one subframe $\mathbf{d}_j$. Formally, if $F_D(T) = \{S_2, \ldots, S_{n_{cc}}\}$ denotes the decomposition of T:

$$\exists\, j \text{ such that } S_j \neq \emptyset \quad \text{and} \quad S_i = \emptyset \;\forall i \neq j. \tag{12}$$

2) Multi-layer TRTZ sequences (TRTZ$_{ml}$): TRTZ sequences that involve $\mathbf{d}_1$ and two or more subframes (e.g., $\mathbf{d}_i$, $\mathbf{d}_j$), where multiple S_i in the decomposition are non-empty:

$$\exists\, i \neq j \text{ such that } S_i \neq \emptyset \text{ and } S_j \neq \emptyset. \tag{13}$$

A particular subclass of TRTZ$_{ml}$, namely TRTZ$_{ml-w1}$, arises when at least one decomposed sequence in a sub-frame has input weight equal to 1, as illustrated in Fig. 3(a,b). If $\#X$ denotes the cardinality of the set X, these sequences satisfy

$$\exists\, i \text{ such that } \#S_i = 1, \tag{14}$$

and typically generate $K/(2\mathcal{L})$ parity bits from each IW-1 $\mathbf{d}_i$.

Accordingly, the complete set of TRTZ sequences $\mathcal{T}$ can be expressed as the union of single-layer and multi-layer subsets:

$$\mathcal{T} = \mathcal{T}_{sl} \cup \mathcal{T}_{ml}, \tag{15}$$

where the dominant low-OW sequences typically stem from low-IW TRTZ sequences. In contrast to conventional TCs, TRTZ$_{ml-w1}$ sequences must be carefully considered during design, as they are invariant to interleaving and can result in low OW depending on the choice of $\mathcal{L}$.

For a given RSC encoder with period p, each IW-2 RTZ sequence of the form $R = \{0, x_1\}$ satisfies the condition $|x_1 - 0| \bmod p = 0$ (see (2)). As a result, there are exactly $\lfloor K/p \rfloor$ such distinct positions in a frame of length K where this condition is satisfied. Owing to the linearity of CCs, each RTZ pattern (i.e., a unique shape) can occur cyclically across all positions in the input frame, resulting in K cyclic shifts per shape. Hence, the total number of IW-2 RTZ sequences in $\mathbf{d}_1$ is $K \cdot \left\lfloor \frac{K}{p} \right\rfloor$, which clearly highlights a quadratic growth with respect to the frame size K. This growth in number of IWs 2 significantly impacts the cardinality of RTZ sequences (see (7)) and thereby increases the likelihood of them leading to low OW TRTZ sequences, hence increasing the size of $\mathcal{T}$.

B. Impact of TRTZ sequences on the choice of $\mathcal{L}$

DPCCC mitigates many of these low-IW patterns, depending on $\mathcal{L}$, which controls the relative sizes of the sets $\mathcal{T}_{sl}$ and $\mathcal{T}_{ml}$. We can distinguish 2 main cases:

1) $\mathcal{L} \bmod p = 0$: For any odd-IW sequence S, the reduction yields $\#F_R(S) = 1$, implying $S \notin \textit{RTZ}_a$. Thus, S is not an RTZ sequence in $\mathbf{d}_1$ (Theorem 1) and $\mathcal{T}_{sl} = \mathcal{T}_{sl}^{\text{even}}$. Moreover, from (8), any even-IW RTZ sequence R_ℓ in $\mathbf{d}_\ell$ for $\ell \in \{2, \ldots, n_{cc}\}$ results in a composed sequence R in $\mathbf{d}_1$ such that

$$\forall x_i \in R,\, \exists\, x_j \in R \text{ with } |x_i - x_j| \bmod p = 0. \tag{16}$$

By (2), this implies that R is also an RTZ sequence in $\mathbf{d}_1$, and thus all such sequences are inherently TRTZ$_{sl}$.

This configuration significantly increases the number of even-IW TRTZ$_{sl}$ sequences, making it highly challenging for the interleaver to avoid low OWs. The difficulty is further amplified compared to classical TCs, as interleaving now operates over the shorter subframe size $K/\mathcal{L}$. Consequently, decompositions satisfying $\mathcal{L} \bmod p = 0$ are excluded from further consideration.

2) $\mathcal{L} \bmod p \neq 0$: When $\mathcal{L}$ is not a multiple of p, an IW-2 TRTZ$_{sl}$ sequence arises only when the separation between two bits in $\mathbf{d}_1$ is a multiple of the least common multiple of p and $\mathcal{L}$, denoted by $\langle p, \mathcal{L} \rangle$. This reduces the number of IW-2 TRTZ$_{sl}$ sequences to $K \cdot \lfloor \frac{K}{\langle p, \mathcal{L} \rangle} \rfloor$, compared to $K \cdot \left\lfloor \frac{K}{p} \right\rfloor$ IW-2 TRTZ sequences in conventional TCs, thereby enhancing the interleaver's ability to avoid low-OW cases. IW-2 and IW-3 TRTZ$_{ml}$ sequences are inherently mitigated by suitable decompositions, as they transform into TRTZ$_{ml-w1}$ sequences (Fig. 3(a,b)) with high OWs. While TRTZ$_{sl}$ sequences with

IW ≥ 3 may still occur, their length extends beyond $3\mathcal{L}$ in $\mathbf{d}_1$—the shortest RTZ length scaled by $\mathcal{L}$—resulting in high OW and low impact on the mHD. Consequently, the search space in (11) can be reduced by excluding them from $\mathcal{T}_{sl}$. Finally, TRTZ$_{ml}$ sequences with IW ≥ 4 may still induce low OW, as illustrated in Fig. 3(c), and must be specifically mitigated by the interleaver.

C. Choice of $\mathcal{L}$

The primary objective of interleaver design in DPCCC is to break low-IW TRTZ sequences yielding low OWs. We restrict our focus to configurations where $\mathcal{L} \bmod p \neq 0$.

While increasing $\mathcal{L}$ mitigates TRTZ$_{sl}$ sequences and reduces the size and impact of $\mathcal{T}_{sl}$ by raising their OW, it simultaneously enlarges $\mathcal{T}_{ml}$ by introducing additional inter-subframe dependencies.

More critically, the choice of $\mathcal{L}$ is constrained by the OW of TRTZ$_{ml-w1}$. A large $\mathcal{L}$ reduces the subframe size and interleaving depth, ultimately degrading the Hamming distance. Consequently, a small $\mathcal{L}$ is preferable for short frames to maximize the mHD, while still being carefully balanced with respect to p and K to preserve interleaver flexibility for effectively suppressing TRTZ$_{ml}$ sequences and optimizing the mHD of the DPCCC.

D. Puncturing mask

Systematic data puncturing has been shown to increase the mHD of TCs, enhancing performance in the error floor region [9]. However, this gain may come at the cost of degraded performance in the waterfall region. To balance this tradeoff, it is essential to selectively puncture carefully chosen systematic bits. For DPCCCs, these bits should be selected such that, after applying the decomposition rule, the punctured positions are evenly distributed across all subframes.

To support data puncturing, each RSC encoder is augmented with an additional forward polynomial, thereby reducing its rate from $1/2$ to $1/3$. This modification enables both systematic and parity puncturing via a puncturing mask, which allows for fine-grained rate adaptation while preserving the structural advantages of the DPCCC. For the simulation results presented in Section V, the rate is set to $\mathcal{R} = 1/3$.

E. Proposed interleaver design methodology

The naive approach of jointly designing all interleavers is computationally prohibitive due to the vast search space. To address this, we propose a coordinate descent strategy, where each interleaver Π_q is optimized iteratively, conditioned on all previously designed interleavers Π_ℓ for $\ell < q$.

This iterative design aims to identify interleaver parameters achieving a mHD exceeding a specified threshold, $d_{\text{threshold}}$, which is incremented after each successful iteration to progressively refine the design.

The method starts by initializing an empty matrix $\boldsymbol{B}$, which stores the best found interleaver configurations. Each row in $\boldsymbol{B}$ corresponds to an interleaver Π_ℓ represented by a vector of size $\lfloor K/\mathcal{L} \rfloor$ containing the interleaved addresses. The minimum distance threshold, $d_{\text{threshold}}$, is initially set to 1 (or higher based on the estimated $d_{\min}$).

Algorithm 1 Proposed interleaver design

```
Initialize: B = [], d_threshold = 1
while stopping criterion not met do
    A ← []
    for ℓ ∈ ⟦2, ..., L + 1⟧ do
        d_min ← 0
        while d_min < d_threshold do
            Search for possible interleaver Π_ℓ
            Estimate d_min
            If no suitable interleaver is found within a predefined
            search time then
                Restart from line 3
            end if
        end while
        Append Π_ℓ as a row to A
    end for
    Update B ← A
    Increment d_threshold ← d_threshold + 1
end while
```

TABLE I: Estimated mHD of LTE TC and the proposed DPCCC using Algorithm 1, across various decomposition factors $\mathcal{L}$ for $K = 128$ and $K = 1024$, with $G_1 = G(1, \frac{15}{13})_8$ and $G_2 = G(1, \frac{15}{13}, \frac{17}{13})_8$.

	$K = 128$		$K = 1024$		$K = 6144$	
	G_1	G_2	G_1	G_2	G_1	G_2
$\mathcal{L}$ = 2	**28**	**32**	**46**	48	50	48
$\mathcal{L}$ = 4	26	31	**46**	**56**	51	60
$\mathcal{L}$ = 8	24	30	45	54	**57**	**72**
$\mathcal{L}$ = 16	18	19	42	47	54	64
LTE	16		27		26	

The interleaver design is carried out iteratively for each subframe $\ell \in [\![2, \mathcal{L} + 1]\!]$, as follows:

1) **Interleaver generation:** Interleaver Π_ℓ is constructed using the almost regular permutation (ARP) structure, with parameters determined as described in [9].
2) **Distance estimation:** Its mHD is estimated using the decoder-independent method from [7], ignoring contributions of encoders $j \in [\![\ell + 1, \mathcal{L} + 1]\!]$.
3) **Validation:** If the estimated mHD is greater than or equal to $d_{\text{threshold}}$, the selected interleaver is considered valid and appended as a new row to matrix $\boldsymbol{A}$. Otherwise, the process is repeated until a valid interleaver is found.

Once all interleavers are designed, they are stored as the best interleaver set in $\boldsymbol{B}$. The process then proceeds iteratively, incrementing $d_{\text{threshold}}$ by one after each full design cycle until a stopping criterion is met.

To prevent infinite loops, a time limit is imposed for the search of each interleaver Π_ℓ; if no suitable interleaver is found within this period, the algorithm restarts from Π_2 using the previous value of $d_{\text{threshold}}$.

V. Results

To evaluate the proposed DPCCC structure, Algorithm 1 was employed to design interleavers for various decomposition factors $\mathcal{L}$ and frame sizes at a code rate of $\mathcal{R} = 1/3$. Two RSC configurations were considered: a single-parity code $G_1 = G(1, \frac{15}{13})_8$ without puncturing, and a double-parity code

$G_2 = G(1, \frac{15}{13}, \frac{17}{13})_8$ with systematic and parity puncturing to preserve the global code rate at $\mathcal{R} = 1/3$. The data puncturing pattern is [10100000], the parity puncturing patterns are respectively [11101111] for the first parity outputs (polynomial $\frac{15}{13}$) and [01011010] for the second parity outputs (polynomial $\frac{17}{13}$). Table I reports the estimated mHD for different DPCCC decompositions, compared against LTE baselines.

For $K = 128$, the highest mHD is achieved with $\mathcal{L} = 2$ for both RSC codes.Increasing $\mathcal{L}$ degrades the mHD limiting interleaver effectiveness. For $K = 1024$, G_1 attains a maximum mHD of 46 with $\mathcal{L} = 2$ and $\mathcal{L} = 4$, while G_2 reaches an mHD of 56 with $\mathcal{L} = 4$. For $K = 6144$, the highest mHD is observed with $\mathcal{L} = 8$, yielding mHDs of 57 for G_1 and 72 for G_2. These results validate the design strategy for selecting $\mathcal{L}$ and demonstrate the impact of systematic puncturing on enhancing mHD. Compared to LTE, all DPCCC configurations provide superior mHD values, with the best gains reaching 75%, 70%, and 119% for $K = 128$, $K = 1024$, and $K = 6144$ respectively using G_1, and 100%, 107%, and 157% using G_2.

Figure 4 presents the FER performance for various DPCCC configurations using G_1 and the best configurations using G_2. Simulations were conducted in an AWGN channel with BPSK modulation and a maximum of 8 max-log-MAP (MLM) decoding iterations at $\mathcal{R} = 1/3$. For benchmarking, we include LTE TCs, 5G low-density parity-check (LDPC) codes—decoded with 20 iterations of the layered offset min-sum algorithm [10]— and polar codes designed using AFF3CT [11] and decoded via successive cancellation list-32 (SCL-32).

Simulation results at high SNRs align with the mHD estimates in Table I. For $K = 128$ with G_1, the $\mathcal{L} = 2$ configuration achieves the best FER, outperforming all baselines.

For $K = 1024$, the configurations $\mathcal{L} = 2$ and $\mathcal{L} = 4$ deliver the best performance. At $K = 6144$, the 5G LDPC outperforms DPCCC G_1 at higher SNRs, while the proposed DPCCC with G_2 surpasses both. Although G_2 exhibits slightly degraded performance at low SNR due to systematic puncturing, it consistently outperforms G_1, LTE, polar, and LDPC codes at higher SNRs. This confirms the effectiveness of the DPCCC structure and interleaver design.

VI. Conclusion

The proposed DPCCC structure significantly increases the mHD, effectively lowering the error floor compared to classical TCs. By decomposing frames and optimizing interleavers, this approach leverages structural and design advantages. The careful selection of $\mathcal{L}$ combined with an iterative design process is crucial for maximizing code performance and ensuring robustness across varying conditions. Simulation results for different frame sizes demonstrate consistent performance gains over LTE and other coding schemes, such as polar and LDPC codes. Furthermore, the DPCCC structure supports independent decoding of subframes, enabling parallel processing and reduced decoding latency. Compared to classical PCCCs, latency can be reduced by a factor of $\mathcal{L}$ when using techniques such as iteration overlap [12].

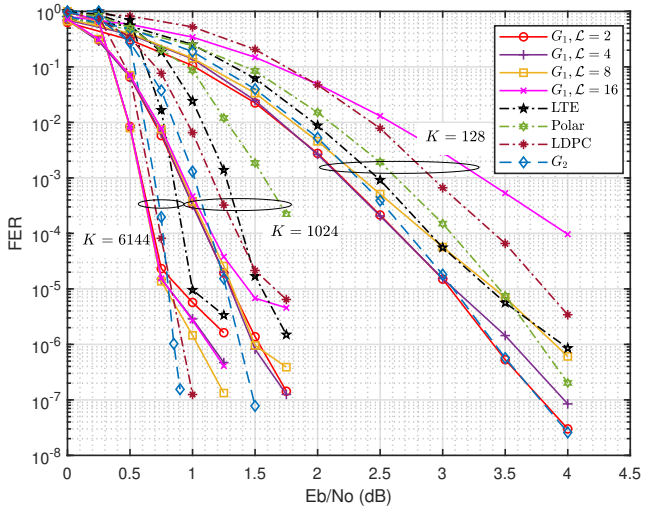

Fig. 4: FER performance of the proposed DPCCC using RSC with generator polynomial $G_1 = G(1, \frac{15}{13})_8$ and the best decomposition factors $\mathcal{L}$ (from Table I) with $G_2 = G(1, \frac{15}{13}, \frac{17}{13})_8$, for various frame sizes. Results are compared against LTE, polar codes decoded via SCL-32, and 5G LDPC decoded using the layered offset min-sum algorithm with 20 iterations. Simulations for LTE and DPCCC assume a maximum of 8 MLM decoding iterations and rate $\mathcal{R} = 1/3$.

References

[1] C. Berrou, A. Glavieux, and P. Thitimajshima, "Near Shannon limit error-correcting coding and decoding: Turbo-codes. 1," in *Proc. of ICC '93 - IEEE Int. Conf. Commun.*, vol. 2, May 1993, pp. 1064–1070 vol.2.

[2] S. Benedetto and G. Montorsi, "Design of parallel concatenated convolutional codes," *IEEE Trans. Commun.*, vol. 44, no. 5, pp. 591–600, May 1996.

[3] H. El Gamal and A. Hammons, "Analyzing the turbo decoder using the gaussian approximation," *IEEE Trans. Inf. Theory*, vol. 47, no. 2, pp. 671–686, Aug. 2001.

[4] 3GPP, "LTE; Evolved universal terrestrial radio access (E-UTRA); Multiplexing and channel coding," TS 36.212 Release 14, 2017.

[5] L. Perez, J. Seghers, and D. Costello, "A distance spectrum interpretation of turbo codes," *IEEE Trans. Inf. Theory*, vol. 42, no. 6, pp. 1698–1709, Nov. 1996.

[6] S. Crozier, P. Guinand, and A. Hunt, "Estimating the Minimum Distance of Large-Block Turbo Codes using Iterative Multiple-Impulse Methods," in *Proc. 4th Int. Symp. Turbo Codes Rel. Topics*, 2006, pp. 1–6.

[7] M. Bazzal, J. Nadal, S. Weithoffer, C. Abdel Nour, and C. Douillard, "Efficient decoder-free minimum distance estimation for concatenated convolutional codes," in *IEEE Veh. Technol. Conf.*, Oslo, July 2025.

[8] R. Garzón-Bohórquez, R. Klaimi, C. Abdel Nour, and C. Douillard, "Mitigating Correlation Problems in Turbo Decoders," in *Proc. Int. Symp. Turbo Codes Rel. Topics (ISTC)*, Hong Kong, Dec. 2018, pp. 1–5.

[9] R. Garzón-Bohórquez, C. Abdel Nour, and C. Douillard, "Protograph-Based Interleavers for Punctured Turbo Codes," *IEEE Trans. Commun.*, vol. 66, no. 5, pp. 1833–1844, Dec. 2018.

[10] D. Hui, S. Sandberg, Y. Blankenship, M. Andersson, and L. Grosjean, "Channel Coding in 5G New Radio: A Tutorial Overview and Performance Comparison with 4G LTE," *IEEE Veh. Technol. Mag.*, vol. 13, no. 4, pp. 60–69, Oct. 2018.

[11] A. Cassagne, O. Hartmann, M. Léonardon, K. He, C. Leroux, R. Tajan, O. Aumage, D. Barthou, T. Tonnellier, V. Pignoly, B. Le Gal, and C. Jégo, "AFF3CT: A Fast Forward Error Correction Toolbox!" *Elsevier SoftwareX*, vol. 10, p. 100345, Oct. 2019.

[12] S. Weithoffer, G. Aousaji, J. Nadal, and C. Abdel Nour, "Iteration Overlap for Low-Latency Turbo Decoding," in *Proc. Int. Symp. Turbo Codes Rel. Topics (ISTC)*, Brest, Sep. 2023, pp. 1–5.